LORENTZ BOOSTED NUCLEON–NUCLEON POTENTIAL APPLIED TO THE $^3\vec{\mathrm{H}}\mathrm{e}(\vec{e}, e'p)pn$ AND $^3\vec{\mathrm{H}}\mathrm{e}(\vec{e}, e'n)pp$ REACTIONS

J. Golak, R. Skibiński, H. Witała

M. Smoluchowski Institute of Physics, Jagellonian University
Reymonta 4, 30-059 Kraków, Poland

W. Glöckle

Institut für Theoretische Physik II, Ruhr Universität Bochum
44780 Bochum, Germany

A. Nogga

Forschungszentrum Jülich, IKP (Theorie), 52425 Jülich, Germany

H. Kamada

Department of Physics, Faculty of Engineering, Kyushu Institute of Technology
1-1 Sensuicho, Tobata, Kitakyushu 804-8550, Japan

(Received December 18, 2006)

We formulate an approximate relativistic framework for an analysis of the $^3\vec{\mathrm{H}}\mathrm{e}(\vec{e}, e'p)pn$ and $^3\vec{\mathrm{H}}\mathrm{e}(\vec{e}, e'n)pp$ reactions. Restricting the rescattering series to one term linear in the two-nucleon ($2N$) t-matrix we incorporate various relativistic features when calculating a nuclear current matrix element. These relativistic ingredients encompass the relativistic ^{3}He wave function based on the concept of the Lorentz boosted nucleon–nucleon potential together with the boosted $2N$ t-matrix, relativistic kinematics and relativistic single-nucleon current operator. This allows us to estimate the magnitude of certain relativistic effects not included in the standard non-relativistic approach. A more complete inclusion of relativity would require that the current operator obeys the covariance equations and the final three-nucleon ($3N$) scattering state with complete final state interactions (FSI) should be properly boosted. We provide some discussion on those issues.

PACS numbers: 21.45.+v, 21.10.Jv, 24.70.+s, 25.10.+s

1. Introduction

Modern three-body calculations allow for a quantitative description of the $3N$ system not only in the bound state [1] but also for the continuum states (see for example [2, 3]). This gives the possibility to test our understanding of the three-body system via interactions with external probes. Among many processes which can be listed here, electron scattering on ^{3}He is of special importance [4, 5]. This process serves as a rich source of information about the nucleon form factors [6–9] and important properties of the ^{3}He nucleus [10–12].

Electron induced breakup of ^{3}He involves many components of the dynamical scenario. Among them the initial ^{3}He and final scattering states must be calculated consistently for the same $3N$ Hamiltonian comprising not only $2N$ but also $3N$ forces. Consequently, also many-body currents consistent with those forces should be taken into account. We refer the reader to [4] for a detailed discussion of the numerical techniques necessary to perform calculations of this reaction. Currently this can be done only nonrelativistically, which is a major restriction and leads to serious difficulties in interpretation of many experiments performed at high energy and momentum transfers. Due to large differences between the nonrelativistic and relativistic kinematics an analysis of such experiments cannot be undertaken within a strictly nonrelativistic framework.

We are not aware of any consistent, relativistic $3N$ scattering calculation. Also in the present paper we report about a less rigorous approach to the description of the $^3\vec{\mathrm{H}}\mathrm{e}(\vec{e}, e'p)pn$ and $^3\vec{\mathrm{H}}\mathrm{e}(\vec{e}, e'n)pp$ processes. This approach does not include all final state interactions (FSI) among the three outgoing nucleons but restricts the rescattering to only one "spectator" pair of nucleons which is assumed not to take part in the photon absorption. There are definitely kinematical regions where such a reaction mechanism seems to be plausible. Furthermore, this approximation was used successfully in the analysis of many experiments (see for example [9, 13]).

We would like to add to this treatment of electron induced breakup of ^{3}He new truly relativistic features. We continue work started in [14], where first steps to extend the Hamiltonian scheme in equal time formulation to $3N$ scattering were made. To this aim the Lorentz boosted nucleon–nucleon (NN) potential which generates the NN T-matrix in a moving frame via a standard Lippmann–Schwinger equation was calculated and applied to the $3N$ bound state problem. In the present paper we show how to obtain the (antisymmetric) $3N$ relativistic wave function and formulate an approximate framework which can be used as a practical tool for an analysis of experimental results, for example in quasi-elastic reactions at high energy and momentum transfers.

We give the reader a detailed derivation of our formalism in Section 2. Section 3 shows our results for the semi-exclusive three-body breakup of ^{3}He. Important missing features required for a more complete treatment of relativity are indicated in Section 4 and illustrated in the Appendix. We end with a brief summary in Section 5.

2. Theory

Before we remind the reader of the most important ideas about the Lorentz boosted NN potential, it seems appropriate to start with the well known nonrelativistic concepts.

The nonrelativistic $2N$ bound state $\mid \psi_b^{(\mathrm{nr})}\rangle$ obeys the equation

$$\mid \psi_b^{(\mathrm{nr})}\rangle = G_0^{(\mathrm{nr})}\, v^{(\mathrm{nr})} \mid \psi_b^{(\mathrm{nr})}\rangle\,, \tag{1}$$

where $v^{(\mathrm{nr})}$ is the nonrelativistic NN potential and $G_0^{(\mathrm{nr})}$ is the nonrelativistic $2N$ free propagator. This can be written in the $2N$ center of mass (c.m.) frame by projecting onto the eigenstate of relative momentum $|\vec{p}>$ ($\vec{p}$ and $-\vec{p}$ are then the individual nucleon momenta)

$$\psi_b^{(\mathrm{nr})}(\vec{p}) = \frac{1}{M_\mathrm{b} - 2m - \vec{p}^{\,2}/m} \int d^3p'\, v^{(\mathrm{nr})}(\vec{p},\vec{p}\,')\, \psi_b^{(\mathrm{nr})}(\vec{p}\,')\,. \tag{2}$$

Here M_b is the $2N$ bound state rest mass and m is the nucleon mass. The corresponding Lippmann–Schwinger equation

$$t^{(\mathrm{nr})} = v^{(\mathrm{nr})} + t^{(\mathrm{nr})} G_0^{(\mathrm{nr})} v^{(\mathrm{nr})} \tag{3}$$

for the t-matrix $t^{(\mathrm{nr})}$ takes in the momentum space the following form

$$t^{(\mathrm{nr})}(\vec{p},\vec{p}\,') \;=\; v^{(\mathrm{nr})}(\vec{p},\vec{p}\,') + \int d^3p''\; \frac{t^{(\mathrm{nr})}(\vec{p},\vec{p}\,'')v^{(\mathrm{nr})}(\vec{p}\,'',\vec{p}\,')}{E_{12}^{\mathrm{nr}} - \vec{p}\,''^{\,2}/m + i\varepsilon}\,, \tag{4}$$

where E_{12}^{nr} is the nonrelativistic $2N$ c.m. kinetic energy. The Galilean invariance of the nonrelativistic scenario guarantees that the relative momentum and Eqs.(1)–(4) remain frame independent.

On the other hand, a relativistic NN potential $v^{(\mathrm{rl})}$ defined in the $2N$ c.m. system appears in the relativistic bound state equation

$$\mid \psi_b^{(\mathrm{rl})}\rangle = G_0^{(\mathrm{rl})} v^{(\mathrm{rl})} \mid \psi_b^{(\mathrm{rl})}\rangle\,, \tag{5}$$

and in the relativistic form of the Lippmann–Schwinger equation

$$t^{(\mathrm{rl})} = v^{(\mathrm{rl})} + t^{(\mathrm{rl})} G_0^{(\mathrm{rl})} v^{(\mathrm{rl})}\,. \tag{6}$$

In the momentum space spanned by eigenstates of the $2N$ c.m. relative momentum $\vec{p}$ the Eqs. (5) and (6) can be written as

$$\psi_b^{(\mathrm{rl})}(\vec{p}) = \frac{1}{M_\mathrm{b} - \omega(\vec{p})} \int d^3p'\, v^{(\mathrm{rl})}(\vec{p},\vec{p}\,')\psi_b^{(\mathrm{rl})}(\vec{p}\,') \tag{7}$$

and

$$t^{(\mathrm{rl})}(\vec{p},\vec{p}\,') = v^{(\mathrm{rl})}(\vec{p},\vec{p}\,') + \int d^3p''\ \frac{t^{(\mathrm{rl})}(\vec{p},\vec{p}\,'')v(\vec{p}\,'',\vec{p}\,')}{E_{12}^{rl} - \omega(\vec{p}\,') + i\varepsilon}\,, \tag{8}$$

where

$$\omega(\vec{p}) \equiv 2\sqrt{m^2 + \vec{p}^{\,2}} \tag{9}$$

and the relativistic $2N$ c.m. energy is denoted by E_{12}^{rl}.

A Lorentz boosted nucleon–nucleon potential $V(\vec{q})$ was introduced in [15, 16] in order to generalize the concept of the relativistic potential for $2N$ systems with the non-zero total momentum $\vec{q}$. It is formally defined via

$$V(\vec{q}) \equiv \sqrt{\left[\omega(\vec{p}) + v^{(\mathrm{rl})}\right]^2 + \vec{q}^{\,2}} - \sqrt{(\omega(\vec{p}))^2 + \vec{q}^{\,2}} \tag{10}$$

and by construction fulfills $V(\vec{q}=0) = v^{(\mathrm{rl})}$. The non-trivial task of obtaining matrix elements $V(\vec{p},\vec{p}\,';\vec{q})$ for arbitrary $\vec{q}$ was accomplished in [14].

With use of the boosted potential, the equation for the relativistic $2N$ bound state moving with the total momentum $\vec{q}$ reads

$$\psi_b^{(\mathrm{rl})}(\vec{p}) = \frac{1}{\sqrt{M_\mathrm{b}^2 + \vec{q}^{\,2}} - \sqrt{\omega(\vec{p})^{\,2} + \vec{q}^{\,2}}} \int d^3p'\, V(\vec{p},\vec{p}\,';\,\vec{q})\,\psi_b^{(\mathrm{rl})}(\vec{p}\,')\,, \tag{11}$$

so the boosted potential allows us to preserve the same structure of the equation as in (2) and (7). Note that $\psi_b^{(\mathrm{rl})}(\vec{p})$ appearing in Eqs. (7) and (11) are identical, *i.e.* the wave function is represented in a way, which does not depend on $\vec{q}$. This is possible because the relative momenta $\vec{p}$ and $\vec{p}\,'$ in both cases are defined in the $2N$ c.m. system.

A formalism for treating the relativistic three-body Faddeev equations was introduced in [15–17]. Since the formal structure of the $3N$ Hamiltonian

$$H = H_0 + \sum_{i<j} V_{ij}\,, \tag{12}$$

with V_{ij} being the boosted two-body force and H_0 the relativistic $3N$ kinetic energy, is the same for relativistic and nonrelativistic approaches, the formal

derivation of the Faddeev equations is also the same in both cases [16]. Thus the Faddeev component $\mid \Phi\rangle$ of the $3N$ relativistic wave function $\mid \Psi\rangle$ generated by interaction V in the $2N$ subsystem obeys

$$\mid \Phi\rangle \;=\; G_0\, T\, P \mid \Phi\rangle\,, \tag{13}$$

where T is the Lorentz boosted T-matrix generated by potential V, G_0 is the relativistic $3N$ free propagator and P is a permutation operator which accounts for the fact that we treat nucleons as identical particles. It is given in terms of the transposition P_{ij} interchanging nucleons "i" with "j": $P \equiv P_{12}P_{23} + P_{13}P_{23}$. The wave function $\mid \Psi\rangle$ follows from the Faddeev component via

$$\mid \Psi\rangle = (1 + P) \mid \Phi\rangle\,. \tag{14}$$

We would like to remark that our $\vec{q}$ is the relative momentum of the spectator in the three-body rest frame. This is to be distinguished from another choice, where $\vec{q}$ is the spectator momentum in any frame. This would lead to a different two-body interaction. With our choice the Poincare generators satisfy the correct commutation relations without the need of an additional three-body interaction. In the second case an additional three-body force is required to recover the commutation relations.

In [16] the boosted T-matrix is constructed from the relativistic $2N$ t-matrices of Eq. (8) in a quite complicated way. Since we have now the Lorentz boosted potential $V(\vec{q})$ at our disposal, we can obtain the boosted (off-shell) T-matrix directly via the Lippmann–Schwinger equation which, when written in the $3N$ c.m. system, takes the form

$$\begin{aligned} T(\vec{p},\vec{p}\,'\,;\,\vec{q}) \;&=\; V(\vec{p},\vec{p}\,'\,;\,\vec{q}) \\ &\quad + \int d^3p\,'' \frac{T(\vec{p},\vec{p}\,''\,;\,\vec{q})\, V(\vec{p}\,'',\vec{p}\,'\,;\,\vec{q})}{E_{3N} - \sqrt{m^2+q^2} - \sqrt{\omega(\vec{p}\,'')^{\,2} + \vec{q}^{\;2}} + i\varepsilon}\,, \end{aligned} \tag{15}$$

where E_{3N} is the total energy of the $3N$ system and $\vec{q}$ is the momentum of the spectator nucleon ($-\vec{q}$ is then a total momentum of the $2N$ subsystem). Due to the following observation, Eq. (15) can be solved as easily as Eq. (4). Namely defining

$$f_q(p) \;\equiv\; \sqrt{\frac{E_{3N} - \sqrt{m^2+q^2} + \sqrt{4m^2+4p^2+q^2}}{4m}}\,, \tag{16}$$

$$v(\vec{p},\vec{p}\,'\,;\,\vec{q}) \;\equiv\; f_q(p)\, V(\vec{p},\vec{p}\,'\!;\,\vec{q})\, f_q(p'\,)\,, \tag{17}$$

$$t(\vec{p},\vec{p}\,'\,;\,\vec{q}) \;\equiv\; f_q(p)\, T(\vec{p},\vec{p}\,'\,;\,\vec{q})\, f_q(p'\,) \tag{18}$$

and

$$p_0^2 \equiv \frac{1}{4}\left(\left(E_{3N} - \sqrt{m^2+q^2}\right)^2 - 4m^2 - q^2\right) \tag{19}$$

we arrive at

$$t(\vec{p},\vec{p}\,';\,\vec{q}) = v(\vec{p},\vec{p}\,';\,\vec{q}) + \int d^3p''\,\frac{t(\vec{p},\vec{p}\,'';\,\vec{q})\,v(\vec{p}\,'',\vec{p}\,';\,\vec{q})}{\frac{p_0^2}{m} - \frac{\vec{p}\,''^2}{m} + i\varepsilon}\,. \tag{20}$$

This looks like a nonrelativistic Lippmann–Schwinger equation (4) and can be solved by the same techniques. Once this equation is solved, Eq. (18) is used to get the $T(\vec{p},\vec{p}\,';\,\vec{q})$ matrix elements. Note that p_0^2 in (20) might be in a general case also negative.

As shown in [14] one needs matrix elements of the relativistic potential $v^{(\mathrm{rl})}$ in order to obtain $V(\vec{p}\,',\vec{p}\,';\,\vec{q})$. The boosted potential is then given by the NN bound state wave function and the half-shell NN t-matrices obtained in the $2N$ c.m. system. The only requirement on $v^{(\mathrm{rl})}$ is that it should describe properly existing $2N$ data set. It is possible to construct $v^{(\mathrm{rl})}$ directly (see for example [18]) or start with a particular modern nonrelativistic potential $v^{(\mathrm{nr})}$ and apply a scale transformation from [19] to generate a phase equivalent relativistic potential $v^{(\mathrm{rl})}$. This second method was criticized in [20] but nevertheless it remains a possibility for practical calculations. Since the general expression for boosted potential $V(\vec{p},\vec{p}\,';\,\vec{q})$ given in [14] is quite complicated it is desirable to find an approximation simplifying numerical calculations. A simple choice is a restriction to the leading order term in a q/ω and v/ω expansion

$$V(\vec{p},\vec{p}\,';\,\vec{q}) \approx v^{(\mathrm{rl})}(\vec{p},\vec{p}\,')\left(1 - \frac{\vec{q}^{\,2}}{2\,\omega(\vec{p})\,\omega(\vec{p}\,')}\right), \tag{21}$$

what turned out to be sufficient for a wide range of $|\,\vec{q}\,|$ values [21] (see also [22]). Such an approximation results in a moving deuteron wave function, a binding energy and S- and D-state probabilities very close to the ones for the deuteron at rest.

In a recent paper [23] an alternative way to arrive directly at the boosted NN t-matrix is given. This is without approximation and appears easy to be implemented. Unfortunately, we got aware of that paper only after finishing this study.

We have now all ingredients to write Eq. (13) in the momentum space. It reads in the $3N$ c.m. system [15–17]

$$\begin{aligned}\Phi(\vec{p},\vec{q}) \;=\; & \frac{1}{E_{\mathrm{b}} - \mathcal{E}(\vec{p},\vec{q})}\int d^3q'\,\frac{T_a(\vec{p},\vec{\pi}(\vec{q}\,',-\vec{q}-\vec{q}\,');\vec{q})}{\mathcal{N}(\vec{q}\,',-\vec{q}-\vec{q}\,')\,\mathcal{N}(-\vec{q}-\vec{q}\,',\vec{q})} \\ & \times \Phi(\vec{\pi}(-\vec{q}-\vec{q}\,',\vec{q}),\vec{q}\,')\,,\end{aligned} \tag{22}$$

where $E_{\rm b}$ is the $3N$ binding energy and the index "a" in the boosted T-matrix indicates that it is the properly antisymmetrized operator with respect to exchanges of two interacting nucleons. The vector $\vec{p}$ represents the relative momentum of two interacting nucleons in their $2N$ c.m. subsystem, and $\vec{q}$ stands for the momentum of the spectator nucleon ($-\vec{q}$ is the total momentum of the interacting $2N$ subsystem). The kinetic energy $\mathcal{E}$ is given by

$$\mathcal{E}(\vec{p},\vec{q}) = \sqrt{\omega\left(\vec{p}\right)^2 + \vec{q}^{\,2}} + \sqrt{m^2 + \vec{q}^{\,2}} - 3m\,. \tag{23}$$

Let us denote the individual momenta of the three nucleons in their $3N$ c.m. system by $\vec{p}_i$, their total energies by E_i, and assume that nucleon 1 is the spectator. Then the relation between the momenta $\vec{p}_2$ and $\vec{p}_3$ of two interacting nucleons and their $2N$ c.m. relative momentum $\vec{p}$, and between spectator momentum $\vec{q}$ and the total momentum $\vec{p}_{23}$ of the interacting $2N$ subsystem reads

$$\vec{q} \;=\; \vec{p}_1 = -\left(\vec{p}_2 + \vec{p}_3\right) \equiv -\vec{p}_{23}\,, \tag{24}$$

$$\vec{p} \equiv \vec{\pi}(\vec{p}_2,\vec{p}_3) \equiv \frac{1}{2}\left(\vec{p}_2 - \vec{p}_3\right) - \frac{1}{2}\vec{p}_{23}\left[\frac{E_2 - E_3}{(E_2+E_3) + \sqrt{(E_2+E_3)^2 - \vec{p}_{23}^{\,2}}}\right]. \tag{25}$$

Relations (24) and (25) can be inverted to express the individual momenta $\vec{p}_2$, $\vec{p}_3$ in the $3N$ c.m. system in terms of the relative momentum $\vec{p}$ of the (23) pair in its $2N$ c.m. system and its total momentum $\vec{p}_{23}$ in the $3N$ c.m. system:

$$\vec{p}_2 \;=\; \vec{p} + \frac{1}{2}\vec{p}_{23} + \frac{\vec{p}\cdot\vec{p}_{23}}{\left[\omega\left(\vec{p}\right) + \sqrt{\omega\left(\vec{p}\right)^2 + \vec{p}_{23}^{\,2}}\right]\omega\left(\vec{p}\right)}\,\vec{p}_{23}\,, \tag{26}$$

$$\vec{p}_3 \;=\; -\vec{p} + \frac{1}{2}\vec{p}_{23} - \frac{\vec{p}\cdot\vec{p}_{23}}{\left[\omega\left(\vec{p}\right) + \sqrt{\omega\left(\vec{p}\right)^2 + \vec{p}_{23}^{\,2}}\right]\omega\left(\vec{p}\right)}\,\vec{p}_{23}\,. \tag{27}$$

The two additional factors $\mathcal{N}(\vec{q}\,',-\vec{q}-\vec{q}\,')$ and $\mathcal{N}(-\vec{q}-\vec{q}\,',\vec{q}\,)$ in Eq. (22) which generally can be written as [16]

$$\mathcal{N}(\vec{p}_2,\vec{p}_3) = \left|\frac{\partial(\vec{p}_2,\vec{p}_3)}{\partial(\vec{p},\vec{p}_{23})}\right|^{\frac{1}{2}} = \left(\frac{4E_2E_3}{\sqrt{(E_2+E_3)^2 - \vec{p}_{23}^{\,2}}(E_2+E_3)}\right)^{\frac{1}{2}}, \tag{28}$$

follow from our assumption on normalization of nucleon momentum eigenstates $\langle\vec{p}_i \mid \vec{p}_i\,'\rangle = \delta(\vec{p}_i - \vec{p}_i\,')$ and the action of the permutation operator P.

In a partial wave representation the relativistic Faddeev Eq. (22) is explicitly given as [16]

$$\phi_\alpha(p,q) \;=\; \frac{1}{E_{\rm b}-\mathcal{E}(p,q)} \sum_{\alpha'\alpha''} \int_0^\infty dq' q'^2 \int_{-1}^{1} dx \, \frac{T_{\alpha\alpha'}(p,\pi_1;q')}{{\pi_1}^{l'}} \times \frac{G_{\alpha'\alpha''}(q,q',x)}{\mathcal{N}_1(q,q',x)\mathcal{N}_2(q,q',x)} \frac{\phi_{\alpha''}(\pi_2,q')}{{\pi_2}^{l''}} \,. \tag{29}$$

The index α comprises a set of quantum numbers (channels)

$$|\,\alpha\rangle = |\,(ls)j(\lambda\tfrac{1}{2})I(jI)J(t\tfrac{1}{2})T\rangle\,, \tag{30}$$

where l, s, j and t are the orbital angular momentum, total spin, total angular momentum and total isospin in the two-body subsystem, respectively. The indices λ, I, J, and T stand for the orbital angular momentum, the total angular momentum of the third particle, the total three-body angular momentum, and the total isospin [24]. $G_{\alpha\alpha'}(q,q',x)$ results from a matrix element of the permutation operator and is given by (note that there is a misprint in Eq. (B2) of Ref. [16])

$$G_{\alpha\alpha'}(q,q',x) \;=\; \sum_k P_k(x) \times \sum_{l_1+l_2=\boldsymbol{l}'_1+l'_2=l'} {p'}^{l_2+l'_2}\, {p'}^{l_1+l'_1} (1+y_1)^{l_2} (1+y_2)^{l'_1}\, g_{\alpha\alpha'}^{kl_1l_2l'_1l'_2} \,. \tag{31}$$

The expressions for π_1, π_2, y_1, y_2, $\mathcal{N}_1(q,q',x)$ and $\mathcal{N}_2(q,q',x)$ as well as other details can be found in [16]. The matrix elements of the permutation operator P that appear in Eqs. (29) and (31) correspond to the form of the permutation operator given in [24]. There are also purely geometrical coefficients $g_{\alpha\alpha'}^{kl_1l_2l'_1l'_2}$ derived (see Eqs. (3.349), (3.352) and (A.19) in that reference). Note that the expressions for the geometrical coefficients are the same in the relativistic and nonrelativistic cases because we neglect the effect of the Wigner spin rotations. This is justified because those effects were found numerically to be of little importance in [21]. Eq. (29) was then solved in [14] with the principal result that the relativistic binding energies are smaller by 0.3–0.45 MeV with respect to the nonrelativistic values based on the same $2N$ potentials.

In many applications the partial wave projected Faddeev components $\phi_\alpha(p,q)$ are not sufficient and we will show now how to obtain the relativistic wave function components $\psi_\alpha(p,q)$ from Eq. (14). To this aim we derive and apply a version of the relativistic operator P "working to the right". As usual it is sufficient to consider only one overlap, for example ${}_1\langle \vec{p}\,\vec{q} \mid \vec{p}\,'\vec{q}\,'\rangle_2$. We restrict ourselves to the $3N$ c.m. system and express the individual momenta $\vec{p}_1$, $\vec{p}_2$ and $\vec{p}_3$ in terms of $\vec{p}$ and $\vec{q}$ using Eqs. (26) and (27)

$$\vec{p}_1 \;=\; \vec{q}, \tag{32}$$

$$\vec{p}_2 \;=\; \vec{p} - \frac{1}{2}\vec{q} + \frac{\vec{p}\cdot\vec{p}}{\left[\omega\left(\vec{p}\right) + \sqrt{\omega\left(\vec{p}\right)^2 + \vec{q}^{\,2}}\right]\omega\left(\vec{p}\right)}\,\vec{q}, \tag{33}$$

$$\vec{p}_3 \;=\; -\vec{p} - \frac{1}{2}\vec{q} - \frac{\vec{p}\cdot\vec{q}}{\left[\omega\left(\vec{p}\right) + \sqrt{\omega\left(\vec{p}\right)^2 + \vec{q}^{\,2}}\right]\omega\left(\vec{p}\right)}\,\vec{q}. \tag{34}$$

Next we calculate the relative momentum of nucleons 3 and 1 in their $2N$ c.m. frame using Eq. (25)

$$\vec{p}\,'' \equiv \vec{\pi}(\vec{p}_3,\vec{p}_1) \equiv \frac{1}{2}\left(\vec{p}_3 - \vec{p}_1\right) - \frac{1}{2}\vec{p}_{31}\,\left[\frac{E_3 - E_1}{(E_3+E_1)+\sqrt{(E_3+E_1)^2-\vec{p}_{31}^{\,2}}}\right], \tag{35}$$

where $\vec{p}_{31} = \vec{p}_3 + \vec{p}_1 = -\vec{p}_2$. As a consequence ${}_1\langle \vec{p}\,\vec{q} \mid \vec{p}\,'\vec{q}\,'\rangle_2$ becomes

$$\begin{aligned}
{}_1\langle \vec{p}\vec{k} \mid \vec{p}\,'\vec{k}\,'\rangle_2 &= \left|\frac{\partial(\vec{p}_2,\vec{p}_3)}{\partial(\vec{p},\vec{p}_{23})}\right|^{\frac{1}{2}} \left|\frac{\partial(\vec{p}\,'',\vec{p}_{31})}{\partial(\vec{p}_3,\vec{p}_1)}\right|^{\frac{1}{2}} \delta^3\left(\vec{p}\,' - \vec{p}\,''(\vec{p},\vec{q})\right)\,\delta^3\left(\vec{q}\,' - \vec{p}_2(\vec{p},\vec{q})\right) \\
&= \left(\frac{4E_2E_3}{(E_2+E_3)\sqrt{(E_2+E_3)^2-\vec{p}_{23}^{\,2}}}\right)^{\frac{1}{2}} \left(\frac{(E_3+E_1)\sqrt{(E_3+E_1)^2-\vec{p}_{31}^{\,2}}}{4E_3E_1}\right)^{\frac{1}{2}} \\
&\quad \times \delta^3\left(\vec{p}\,' - \vec{p}\,''(\vec{p},\vec{q})\right)\,\delta^3\left(\vec{q}\,' - \vec{p}_2(\vec{p},\vec{q})\right) \\
&\equiv M(\vec{p},\vec{q})\,\delta^3\left(\vec{p}\,' - \vec{p}\,''(\vec{p},\vec{q})\right)\,\delta^3\left(\vec{q}\,' - \vec{p}_2(\vec{p},\vec{q})\right).
\end{aligned} \tag{36}$$

The scalar function $M(\vec{p},\vec{q})$ actually depends on the magnitudes $\mid \vec{p}\mid$, $\mid \vec{q}\mid$ and the scalar product $x \equiv \hat{p}\cdot\hat{q}$. Again it is easy to recover the nonrelativistic limit of this overlap:

$$M(\vec{p},\vec{q}\,) \;\to\; 1\,, \tag{37}$$

$$\vec{p}\,''(\vec{p},\vec{q}\,) \;\to\; -\frac{1}{2}\vec{p}-\frac{3}{4}\vec{q}, \tag{38}$$

$$\vec{p}_2(\vec{p},\vec{q}\,) \;\to\; \vec{p}-\frac{1}{2}\vec{q}. \tag{39}$$

Having obtained Eq. (36) it is then straightforward to calculate the matrix elements of the permutation operator P in our standard basis [24]

$$\langle p\,q\,\alpha \mid P \mid p'\,q'\,\alpha'\rangle = \int\limits_{-1}^{1} dx\,\frac{\delta(p^{'}-\tilde{p})}{\tilde{p}^{\,l^{'}+2}}\,\frac{\delta(q^{'}-\tilde{q})}{\tilde{q}^{\,\lambda^{'}+2}}\,\tilde{G}_{\alpha\alpha'}(p,q,x)\,M(p,q,x)\,, \tag{40}$$

where

$$\tilde{p} \;\equiv\; \sqrt{\frac{1}{4}\,p^2(1-g)^2+\frac{9}{16}q^2(1+h)^2+\frac{3}{4}\,pqx(1-g)(1+h)}\,, \tag{41}$$

$$\tilde{q} \;\equiv\; \sqrt{p^2+\frac{1}{4}q^2(1+2f)^2-pqx(1+2f)}\,,$$

$$\begin{aligned}\tilde{G}_{\alpha\alpha'}(p,q,x) \;&=\; \sum_k P_k(x) \sum_{l'_1+l'_2=l'} \sum_{\lambda'_1+\lambda'_2=\lambda'} p^{\,l'_1+\lambda'_1}\,q^{\,l'_2+\lambda'_2} \\ &\quad\times (1-g)^{l'_1}\,(1+h)^{l'_2}\,(1+2f)^{\lambda'_2}\,\tilde{g}_{\alpha\alpha'}^{\,kl'_1l'_2\lambda'_1\lambda'_2}\,,\end{aligned} \tag{42}$$

$$f \;\equiv\; \frac{-pqx}{\left(2\sqrt{m^2+p^2}+\sqrt{4m^2+4p^2+q^2}\right)2\sqrt{m^2+p^2}}\,, \tag{43}$$

$$g \;\equiv\; \frac{E_3-E_1}{(E_3+E_1)+\sqrt{(E_3+E_1)^2-\vec{p}_{31}^{\,2}}}\,, \tag{44}$$

and finally

$$h \equiv -\frac{2}{3}f+\frac{1}{3}g+\frac{2}{3}fg\,. \tag{45}$$

The purely geometrical quantity $\tilde{g}_{\alpha\alpha'}^{\,kl'_1l'_2\lambda'_1\lambda'_2}$ is strictly the same (under the neglection of the Wigner spin rotations) as we use for example in [25]. Consequently, the $3N$ bound state wave function components can be easily calculated.

We would like to give the reader an example of the difference between the nonrelativistic and relativistic wave function and show the single-nucleon momentum distribution in Fig. 1. We see that differences visible on a logarithmic plot appear only for $q \geq 3$ fm^{-1}. Most important effects are just due to the relativistic kinematics. The approximation given in Eq. (21) does a very good job since the dashed and solid lines nearly overlap. The boost effect is visible for $q \geq 6$ fm^{-1}. The results presented in Fig. 1 and all other results in this paper were obtained with the CD Bonn NN potential [26]. Based on our experience, see for example [27], we expect little sensitivity of our results to the choice of a modern high precision NN potential.

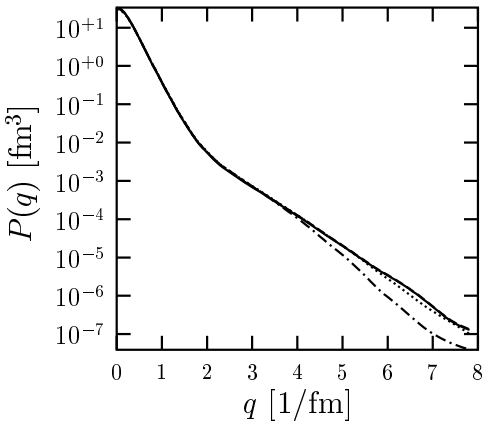

Fig. 1. The single-nucleon momentum distribution for the $3N$ bound state. The curves correspond to strictly nonrelativistic (dash-dotted), relativistic with no boost effects in the T-matrix (dotted), relativistic with approximate boost effects in the T-matrix according to Eq. (21) (dashed) and fully relativistic calculations (solid).

3. Results for the $^3\vec{\mathrm{H}}\mathrm{e}(\vec{e}, e'p)pn$ and $^3\vec{\mathrm{H}}\mathrm{e}(\vec{e}, e'n)pp$ processes

We will start this section with a brief derivation of the nuclear matrix elements corresponding to Fig. 2. Here we do not take FSI among the three outgoing nucleons fully into account. In the A_1 diagram, which we call the plane wave impulse approximation (PWIA) in this paper, FSI is totally neglected. In the A_2 diagram FSI is restricted only to one pair of nucleons. We will denote the approximation corresponding to the sum of diagrams A_1 and A_2 by FSI23. The laboratory frame coincides with the initial $3N$ c.m. system so the projection of the relativistic wave function on the space of the individual momenta $\vec{p}_i$ reads

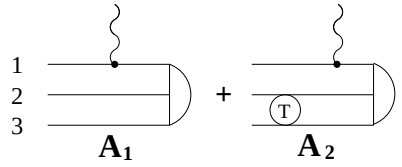

Fig. 2. Diagrammatic representation of the three-body breakup of ^{3}He. The curly lines denote the photon coupling to nucleon 1. The large semi-circles depict the initial ^{3}He bound state. While the diagram A_1 neglects all the final state interactions among the three final nucleons, in the diagram A_2 the boosted scattering operator T acts only in the subsystem (23).

$$\langle \vec{p}_1\, \vec{p}_2\, \vec{p}_3 \mid \Psi_b \rangle = \frac{1}{\mathcal{N}(\vec{p}_2, \vec{p}_3)} \langle \vec{\pi}(\vec{p}_2, \vec{p}_3), \vec{p}_1 \mid \Psi_b \rangle \,. \tag{46}$$

Assuming the action of the single nucleon current operator, the amplitude A_1 takes a very simple form

$$A_1 = \langle \vec{p}_1 m_1 \nu_1 \vec{p}_2 m_2 \nu_2 \vec{p}_3 m_3 \nu_3 \mid j(\vec{Q}, 1) \mid \Psi_b M M_T \rangle \,, \tag{47}$$

where m_i (ν_i) are spin (isospin) projections of the outgoing nucleons. The spin (isospin) magnetic quantum number of the initial $3N$ bound state is denoted by M (M_T). ($M_T = \frac{1}{2}$ for the ^{3}He nucleus.) The single nucleon current $j(\vec{Q}, 1)$ acts only on the nucleon 1. One proceeds by inserting single nucleon intermediate states and using (46)

$$\begin{aligned} A_1 \;=\; & \delta\Big(\vec{p}_1 + \vec{p}_2 + \vec{p}_3 - \vec{Q}\Big) \sum_{m_1{}'} j\Big(\vec{p}_1, \vec{p}_1 - \vec{Q}; m_1, m_1{}'; \nu_1\Big) \\ & \times \Big\langle \vec{p}\, \vec{q}\, m_1{}' m_2 m_3 \nu_1 \nu_2 \nu_3 \Big| \Psi_b M M_T \Big\rangle \; \frac{1}{\mathcal{N}(\vec{p}_2, \vec{p}_3)} \,, \end{aligned} \tag{48}$$

where $\vec{p} \equiv \vec{\pi}(\vec{p}_2, \vec{p}_3)$, and $\vec{q} \equiv \vec{p}_1 - \vec{Q}$. Finally we use the partial wave decomposition of the bound state in the basis $\mid pq\alpha \rangle$ and arrive at

$$\begin{aligned} A_1 = {} & \delta(\vec{p}_1 + \vec{p}_2 + \vec{p}_3 - \vec{Q}) \delta_{\nu_1 + \nu_2 + \nu_3, M_T} \\ & \times \frac{1}{\mathcal{N}(\vec{p}_2, \vec{p}_3)} \sum_{m_1{}'} j(\vec{p}_1, \vec{p}_1 - \vec{Q}; m_1, m_1{}'; \nu_1) \\ & \times \sum_{\alpha'} \sum_{\mu'} C(j', I', \tfrac{1}{2}; \mu', M - \mu', M) C(l', s', j'; \mu' - m_2 - m_3, m_2 + m_3, \mu') \\ & \times C(\tfrac{1}{2}, \tfrac{1}{2}, s'; m_2, m_3, m_2 + m_3)\, C(\lambda', \tfrac{1}{2}, I'; M - \mu' - m_1{}', m_1{}', M - \mu') \\ & \times C(t', \tfrac{1}{2}, \tfrac{1}{2}; \nu_2 + \nu_3, \nu_1, \nu_1 + \nu_2 + \nu_3)\; C(\tfrac{1}{2}, \tfrac{1}{2}, t'; \nu_2, \nu_3, \nu_2 + \nu_3) \\ & \times Y_{l', \mu' - m_2 - m_3}(\hat{p})\; Y_{\lambda', M - \mu' - m_1{}'}(\hat{q})\; \langle pq\alpha' \mid \Psi_b \rangle \,. \end{aligned} \tag{49}$$

The amplitude A_2 additionally contains the free $3N$ propagator G_0 and the (half-shell) boosted scattering operator T acting in the (23) subsystem

$$\begin{aligned}
A_2 &= \langle \vec{p}_1 m_1 \nu_1 \vec{p}_2 m_2 \nu_2 \vec{p}_3 m_3 \nu_3 \mid T\, G_0\, j(\vec{Q},1) \mid \Psi_b M M_T \rangle \\
&= \delta(\vec{p}_1+\vec{p}_2+\vec{p}_3-\vec{Q})\ \delta_{\nu_1+\nu_2+\nu_3,M_T}\ \delta_{\nu_1,\nu_1'}\ \frac{1}{\mathcal{N}(\vec{p}_2,\vec{p}_3)} \\
&\quad \times \sum_{m_1'} j(\vec{p}_1,\vec{p}_1-\vec{Q};m_1,m_1';\nu_1) \\
&\quad \times \int d\vec{p}\,' \sum_{m_2',m_3'} \sum_{\nu_2',\nu_3'} \delta_{\nu_2+\nu_3,\nu_2'+\nu_3'} \\
&\quad \times \langle \vec{p} m_2 m_3 \nu_2 \nu_3 \mid T(\vec{p}_2+\vec{p}_3) \mid \vec{p}\,' m_2' m_3' \nu_2' \nu_3' \rangle \\
&\quad \times \frac{1}{E_2+E_3-\sqrt{4m^2+4\vec{p}\,'^{\,2}+(\vec{Q}-\vec{p}_1)^{\,2}}+i\varepsilon} \\
&\quad \times \langle \vec{p}\,'\, \vec{q}\, m_1' m_2' m_3' \nu_1' \nu_2' \nu_3' \mid \Psi_b M M_T \rangle\,. \qquad (50)
\end{aligned}$$

In the final step both the bound state wave function and the T-matrix are given in the partial wave basis, which yields

$$\begin{aligned}
A_2 &= \delta(\vec{p}_1+\vec{p}_2+\vec{p}_3-\vec{Q})\ \delta_{\nu_1+\nu_2+\nu_3,M_T} \frac{1}{\mathcal{N}(\vec{p}_2,\vec{p}_3)} \\
&\quad \times \sum_{m_1'} j(\vec{p}_1,\vec{p}_1-\vec{Q};m_1,m_1';\nu_1) \\
&\quad \times \sum_{lsj\mu t} C(l,s,j;\mu-m_2-m_3,m_2+m_3,\mu)\, C(\tfrac{1}{2},\tfrac{1}{2},s;m_2,m_3,m_2+m_3) \\
&\quad \times C(t,\tfrac{1}{2},\tfrac{1}{2};\nu_2+\nu_3,\nu_1,\nu_1+\nu_2+\nu_3)\ C(\tfrac{1}{2},\tfrac{1}{2},t;\nu_2,\nu_3,\nu_2+\nu_3) \\
&\quad \times Y_{l,\mu-m_2-m_3}(\hat{p}) \sum_{\bar{l}} \sum_{\alpha'} \delta_{l'\bar{l}}\, \delta_{s's}\, \delta_{j'j}\, \delta_{t't}\, C(j,I',\tfrac{1}{2};\mu,M-\mu,M) \\
&\quad \times C(\lambda',\tfrac{1}{2},I';M-\mu-m_1',m_1',M-\mu)\ Y_{\lambda',M-\mu-m_1'}(\hat{q}) \\
&\quad \times \int dp'\, p'^{\,2} \langle p(ls)jt \mid T(\vec{Q}-\vec{p}_1) \mid p'(l's')jt \rangle \langle p'q\alpha' \mid \Psi_b \rangle \\
&\quad \times \frac{1}{E_2+E_3-\sqrt{4m^2+4\vec{p}\,'^{\,2}+(\vec{Q}-\vec{p}_1)^{\,2}}+i\varepsilon}\,. \qquad (51)
\end{aligned}$$

The single nucleon current matrix elements $j(\vec{p}_1,\vec{p}_1\,';m_1,m_1';\nu_1)$ (ν_1 decides whether the photon couples to a proton or to a neutron) are taken

completely relativistically, *i.e.*

$$j(\vec{p},\vec{p}\,';m_1,{m_1}') \equiv j^{\mu}(\vec{p},\vec{p}\,';m_1,{m_1}')$$
$$= \sqrt{\frac{m}{\sqrt{m^2+p^2}}}\sqrt{\frac{m}{\sqrt{m^2+p'^2}}}\bar{u}(pm_1)\left(F_1\gamma^{\mu}+iF_2\sigma^{\mu\nu}(p-p')_{\nu}\right)u(p'{m_1}'), \tag{52}$$

where u are Dirac spinors. $F_1(p'-p)^2)$ and $F_2(p'-p)^2)$ are Pauli and Dirac nucleon form factors, respectively. In this paper we used the Höhler parametrization for the nucleon electromagnetic form factors [28].

Please note that in general keeping the complete final state interaction the final state wave function has to be boosted. We refer to Sec. 4, where an approximate $3N$ Hamiltonian in a moving frame is proposed. In our approximation it is sufficient to use just the relativistic kinematics and boost the two-body t-matrix.

In this section the results for the three-body breakup will be discussed. We assume the reference frame for which the three-momentum transfer $\vec{Q} \equiv \vec{k}-\vec{k}\,'$ is parallel to $\hat{z}$, $\hat{y} \equiv (\vec{k}\,'\times\vec{k})/(|\,\vec{k}\,'\times\vec{k}\,|)$, and $\hat{x}=\hat{y}\times\hat{z}$. Here $\vec{k}$ and $\vec{k}\,'$ are the initial and final electron momenta. The exclusive cross section for the $e+{}^3\mathrm{He}\to e'+p+p+n$ reaction has the form [29]

$$\begin{aligned} d\sigma(\vec{S},h) \;=\; & \sigma_{\mathrm{Mott}}\,\{(v_{\mathrm{L}}W_{\mathrm{L}}+v_{\mathrm{T}}W_{\mathrm{T}}+v_{\mathrm{TT}}W_{\mathrm{TT}}+v_{\mathrm{TL}}W_{\mathrm{TL}}) \\ & +\; h\,(v_{\mathrm{T}'}W_{\mathrm{T}'}+v_{\mathrm{TL}'}W_{\mathrm{TL}'})\,\}\;\delta\left(k+m_{^3\mathrm{He}}-k'-E_1-E_2-E_3\right) \\ & \times\delta\left(\vec{k}-\vec{k}\,'-\vec{p}_1-\vec{p}_2-\vec{p}_3\right)\,d^3\vec{k}\,'\,d^3\vec{p}_1\,d^3\vec{p}_2\,d^3\vec{p}_3\,, \end{aligned} \tag{53}$$

where σ_{Mott} and all v_i are analytically given kinematical factors, h is the helicity of the incoming electron and $\vec{S}$ represents the initial ^{3}He spin direction. The electron mass is neglected and $m_{^3\mathrm{He}}$ denotes the ^{3}He mass. The response functions W_i, which contain the whole dynamical information, are constructed from the nuclear current matrix elements taken between the initial bound state and the final scattering state. Using Eq. (53) three observables which we consider in this paper can be easily constructed. The first one is the unpolarized sixfold differential cross section

$$\begin{aligned} \frac{d^6\sigma}{dk'd\hat{k}'\,dE_1\,d\hat{p}_1} \;=\; & \tfrac{1}{2}\sum_{m_S}\sum_{m_1,m_2,m_3}\mathcal{C}\int d\hat{p}\,\mathcal{J}\,p_1E_1\,\frac{1}{4}(E_2+E_3)\,p \\ & \times\sigma_{\mathrm{Mott}}\,(v_{\mathrm{L}}W_{\mathrm{L}}+v_{\mathrm{T}}W_{\mathrm{T}}+v_{\mathrm{TT}}W_{\mathrm{TT}}+v_{\mathrm{TL}}W_{\mathrm{TL}})\;, \end{aligned} \tag{54}$$

where m_S, m_1, m_2, m_3 are spin projections of the initial ^{3}He and of the three outgoing nucleons. The relativistic relative momentum $\vec{p}\equiv p\hat{p}$ is defined in

Eq. (25). The additional factor $\mathcal{C} = \frac{1}{2}$ is necessary only if the observed particle is a neutron (the two not detected particles are then identical). Note that we changed variables according to [16]

$$d^3\vec{p}_1\, d^3\vec{p}_2\, d^3\vec{p}_3 = \mathcal{J}\, d^3\vec{p}_1\, d^3\vec{p}_{23}\, d^3\vec{p}\,, \tag{55}$$

in order to simplify integrations over the unobserved parameters of the final $3N$ system. The kinematical factors in Eq. (54) simplify significantly in the nonrelativistic limit

$$\vec{p} \to \tfrac{1}{2}\,(\vec{p}_2 - \vec{p}_3\,)\;, \qquad E_i \to m\,, \qquad \mathcal{J} \to 1\,. \tag{56}$$

The second and third observables we investigate here are special cases of the helicity asymmetry $A(\vec{S})$

$$A(\vec{S}\,) \equiv \frac{\sigma(\vec{S}, h=+1) - \sigma(\vec{S}, h=-1)}{\sigma(\vec{S}, h=+1) + \sigma(\vec{S}, h=-1)}\,, \tag{57}$$

under the same kinematical conditions as the unpolarized cross section in Eq. (54) and obtained from the corresponding polarized semi-exclusive cross sections $\sigma(\vec{S}, h)$. We consider $A_{\parallel}$ for $\vec{S} \parallel \hat{z}$ and $A_{\perp}$ for $\vec{S} \parallel \hat{x}$. Further we stick to the so-called parallel kinematics, for which the finally observed nucleon is ejected parallel to $\vec{Q}$. In this case $W_{\rm TT} = W_{\rm TL} = 0$. This choice of kinematical conditions is optimal for the FSI23 approximation. We can expect that under these kinematics, at least for high energies, the reaction mechanism is dominated by the processes depicted in Fig. 2.

Our nonrelativistic framework [4] allows us to calculate the initial ^{3}He and final scattering states consistently using any $3N$ realistic Hamiltonian and including also many-body current operators. There is no such relativistic dynamical framework available at the moment and in this paper we would like to study what are the different effects when some nonrelativistic elements are replaced by their relativistic counterparts. We focus on the approximation depicted in Fig. 2 and calculate the matrix elements corresponding to diagrams A_1 and A_2, first strictly non-relativistically, secondly using a mixed approach [13] with the nonrelativistic t-matrix and wave functions but employing relativistic kinematics and the relativistic single nucleon current operator. Finally, we use consistently the relativistic $3N$ bound state, kinematics, the boosted T-matrix and the relativistic single nucleon current operator, as described in Sec. 2.

We chose eight electron kinematics (see Fig. 3 and Table I), characterized by the same electron beam energy (E=2000 MeV) and different values of the energy (ω) and momentum ($Q = \mid \vec{Q} \mid$) transfers. For some of them full inclusion of FSI is possible within our nonrelativistic framework, since the

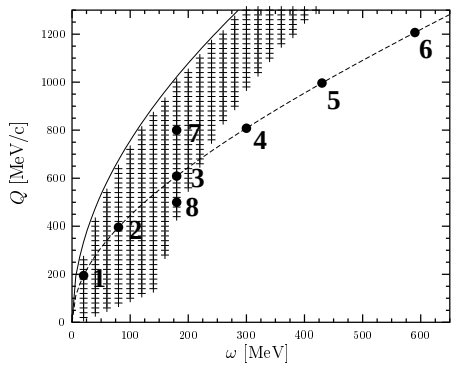

Fig. 3. Eight electron kinematics ((ω, Q) points) considered in the present paper are marked as full circles. The shaded area shows the (ω, Q) points for which the $3N$ c.m. kinetic energy is smaller than the pion mass. The solid lined corresponds to elastic electron scattering on ^{3}He and the dashed line to the quasi-free scattering condition (scattering on a free nucleon).

$3N$ c.m. energy does not allow for pion production. In that case we always used the nonrelativistic current operator. We will thus check to what extent the FSI23 approximation might be sufficient and then concentrate more on different relativistic effects within this simplified relativistic framework. For more detailed discussion of the validity of the FSI23 approximation see [30].

TABLE I

Parameters of the eight electron kinematics studied in this paper: the electron scattering angle θ_e, the outgoing electron energy E', the energy transfer ω, the magnitude of the three-momentum transfer Q, the relativistic ($E^{3N}_{\rm c.m.}$ (rel)) and nonrelativistic ($E^{3N}_{\rm c.m.}$ (nrl)) kinetic c.m. $3N$ energies.

electron kinematics	θ_e [deg]	E' [MeV]	ω [MeV]	Q [MeV/c]	$E^{3N}_{\rm c.m.}$(rel) [MeV]	$E^{3N}_{\rm c.m.}$(nrl) [MeV]
k1	5.6	1980	20	194.8	5.6	5.5
k2	11.4	1920	80	395.8	45.0	44.5
k3	17.5	1820	180	608.6	109.7	106.5
k4	23.5	1700	300	808.3	185.4	176.3
k5	29.4	1570	430	996.2	265.3	246.1
k6	36.5	1410	590	1206.7	360.9	323.8
k7	23.6	1820	180	800.0	63.2	58.7
k8	14.0	1820	180	500.0	130.2	127.9

The kinematics k1–k6 are chosen along the quasi-elastic scattering line. The additional kinematics k7 and k8 are chosen above and below the quasi-elastic line in order to identify differences with respect to the kinematics that belong to the quasi-elastic scattering group.

For the first two figures (Fig. 4 and Fig. 5) we show the parallel helicity asymmetry $A_{\parallel}$ both for the neutron and proton knockout. In most cases the FSI23 approximation is not sufficient, *i.e.* the nonrelativistic FSI23 curve lies far away from the nonrelativistic prediction taking FSI fully into account. The latter reveals very often much a more complicated behavior contrary to the rather simple shapes of the FSI23 predictions. This FSI23 approximation turns out to be satisfactory (however not always) only at the upper end of the energy spectrum for higher magnitudes of the three-momentum transfers. It is interesting to notice that the contribution from the A_2 diagram is very small for the k1 kinematics in the neutron case. Here the PWIA and all FSI23 curves overlap. That does not mean, however, that all FSI is negligible in this case. Already the symmetrization in the plane wave predictions changes the picture significantly and the results with full inclusion of FSI are still very different.

The relativistic effects (the spread among the three FSI23 predictions) are generally most evident not for the maximal energy of the ejected nucleon, where the (23) subsystem c.m. energy is very small, but rather in the middle of the nucleon energy range. Generally, the mixed approach to the FSI23 calculation is closer to the relativistic result than its fully non-relativistic partner. Especially for the k7 kinematics the difference between the relativistically and non-relativistically calculated maximal energy of the knocked out nucleon is clearly visible. For the neutron knockout at the k3 and k4 kinematics the asymmetries tend to reach specific values which depend only on the neutron magnetic form factors and trivial kinematic factors. This corresponds very closely to electron scattering on a free, fully polarized neutron at rest and was suggested as a way to access the important neutron property, since there is no free neutron target in nature. Note the big differences between the results for the k3, k7 and k8 kinematics which all belong to the same energy transfer ω but have different magnitude Q of the three momentum transfer.

These differences are even more true for the perpendicular helicity asymmetry $A_{\perp}$ displayed in Figs. 6 and 7. For this observable, especially in the case of the neutron knockout, FSI23 predictions come close to the results fully employing FSI only for the k3 kinematics, which lies on the quasi-elastic scattering curve. The FSI23 predictions lie lower (k7) or higher (k8) than the results based on the more complete dynamical model. Also for this asymmetry the PWIA and FSI23 predictions take very simple shapes at the first two kinematics, while the full inclusion of FSI leads to more complicated structures. The perpendicular asymmetry for the neutron knockout

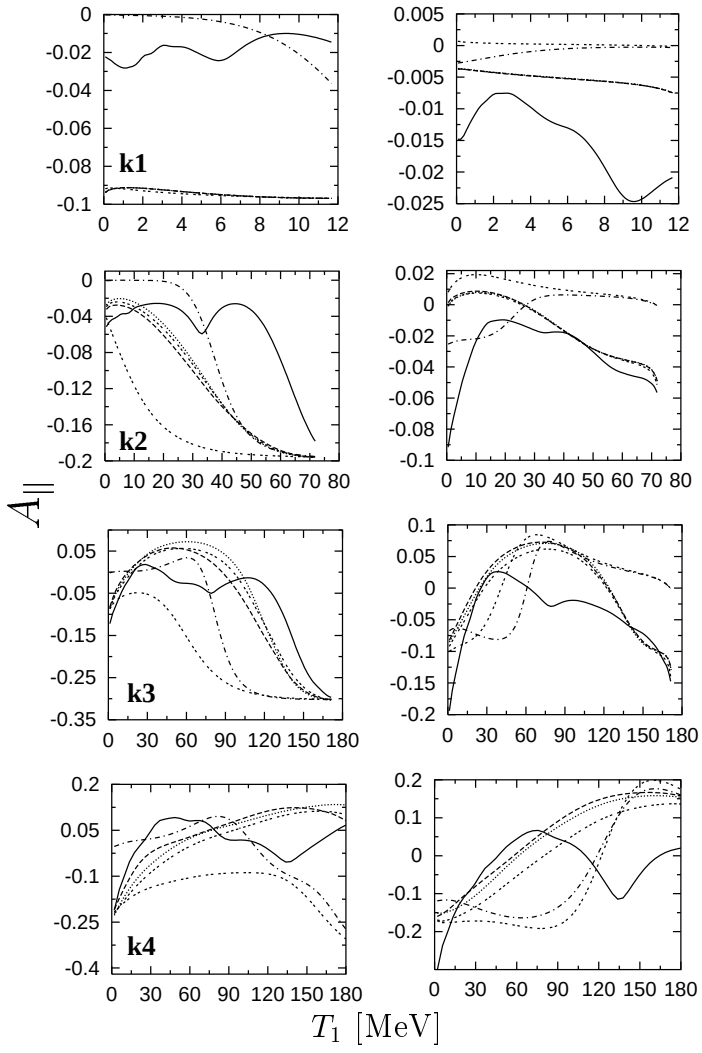

Fig. 4. The parallel asymmetry $A_{\|}$ for the neutron (left panel) and proton (right panel) ejection in the virtual photon direction as a function of the emitted nucleon kinetic energy $T_1 \equiv E_1 - m$ for the first four electron kinematics from Table I. The double dashed line shows the nonrelativistic PWIA prediction and the dash-dotted line the nonrelativistic symmetrized PWIA (PWIAS) prediction. Further we show the strictly nonrelativistic FSI23 results (triple dashed line), the FSI23 predictions with some relativistic features as described in the text (dotted line), and the consistent relativistic FSI23 results (dashed line). Finally the prediction with full inclusion of FSI is represented by the solid line.

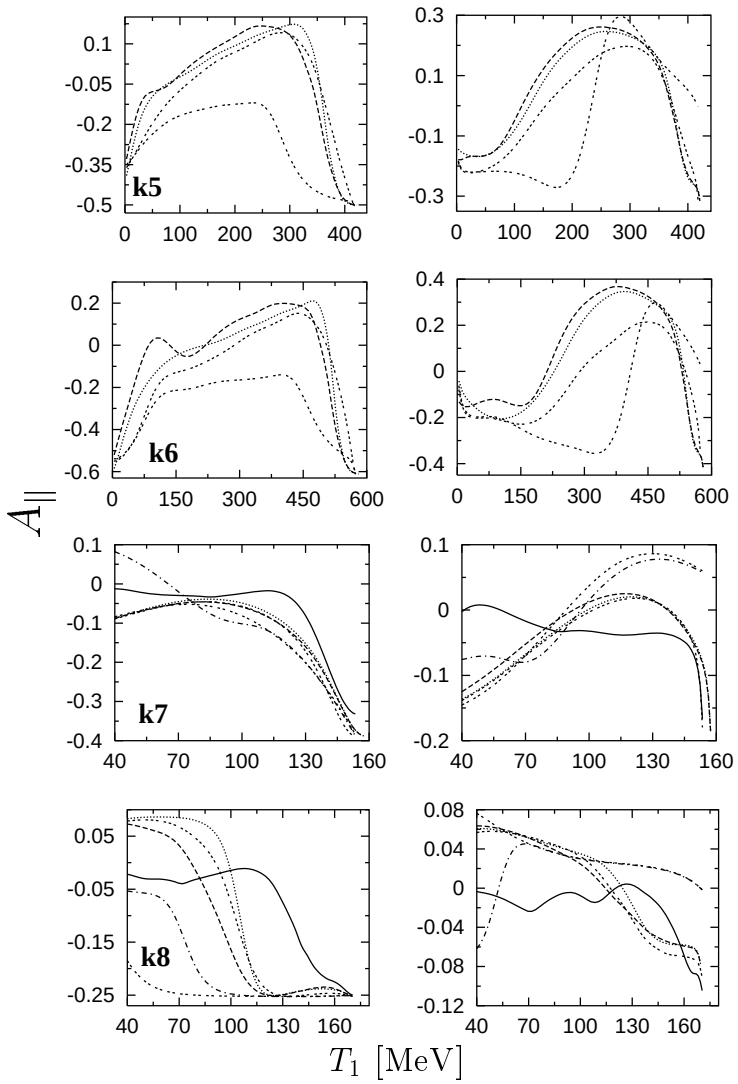

Fig. 5. The same as in Fig. 4 for the remaining four electron kinematics from Table I. The PWIAS prediction and the one with full FSI are missing for the k5 and k6 kinematics.

process is very sensitive to the neutron electric form factor so also in this case the values for the maximal neutron energies, especially at the k3 and k4 kinematics, are determined predominantly by the neutron electric form factor values. This explains why in the neutron case the parallel asymmetry is much bigger than the perpendicular one.

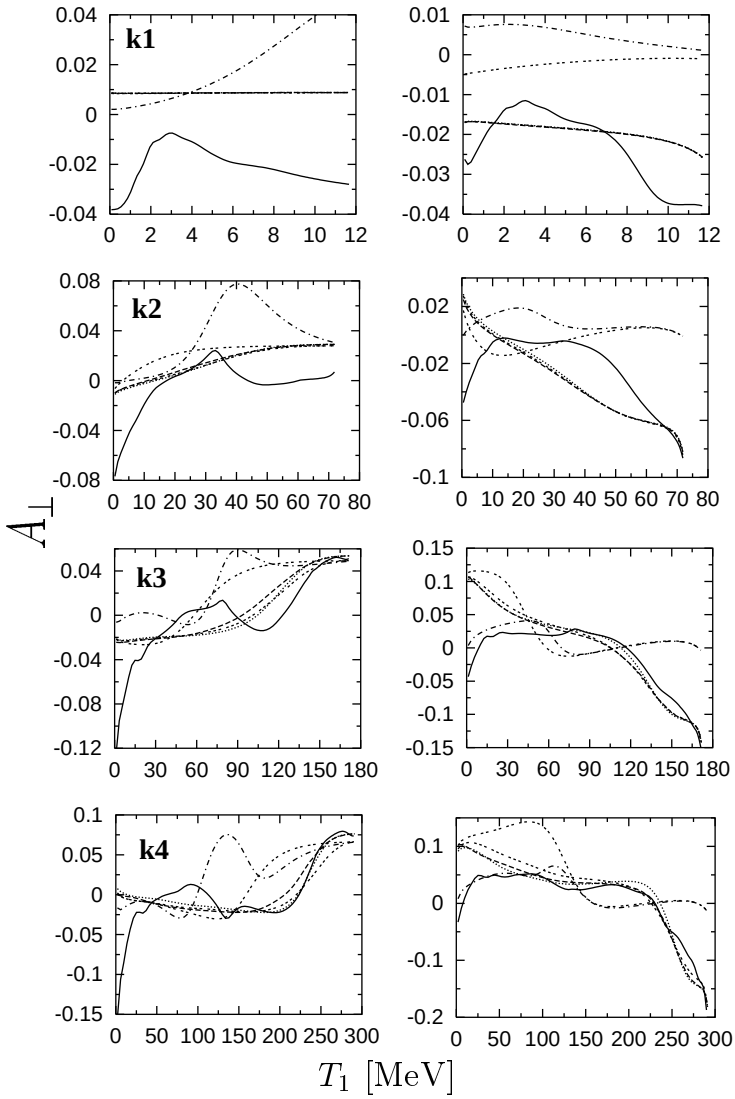

Fig. 6. The same as in Fig. 4 for the perpendicular asymmetry $A_\perp$.

For the k5 and k6 kinematics there is a clear gap between the pure nonrelativistic FSI23 result and the predictions employing relativistic kinematics and the relativistic current operator. This is partly due to the arguments of the electromagnetic form factors, which differ for these two approaches. In the nonrelativistic case we simply take $\omega^2 - \vec{Q}^2$ which does not correspond to the true four-momentum transfer felt by the nucleon. In the relativistic

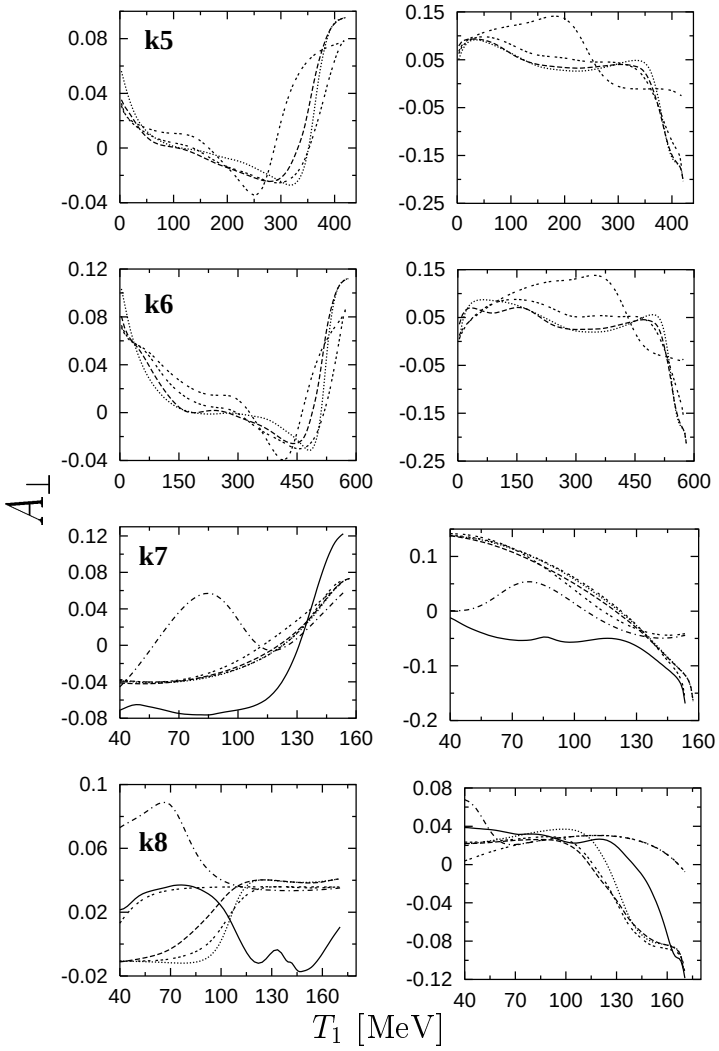

Fig. 7. The same as in Fig. 6 for the remaining four electron kinematics from Table I. The PWIAS prediction and the one with full FSI are missing for the k5 and k6 kinematics.

case we (exactly) account for the four momentum transferred to the nucleon using the following form

$$\left(\sqrt{m^2+(\vec{p}+\vec{Q})^{\,2}}-\sqrt{m^2+\vec{p}^{\,2}}\right)^2-\vec{Q}^{\,2}\,, \tag{58}$$

where $\vec{p}$ is the nucleon momentum prior to photon absorption.

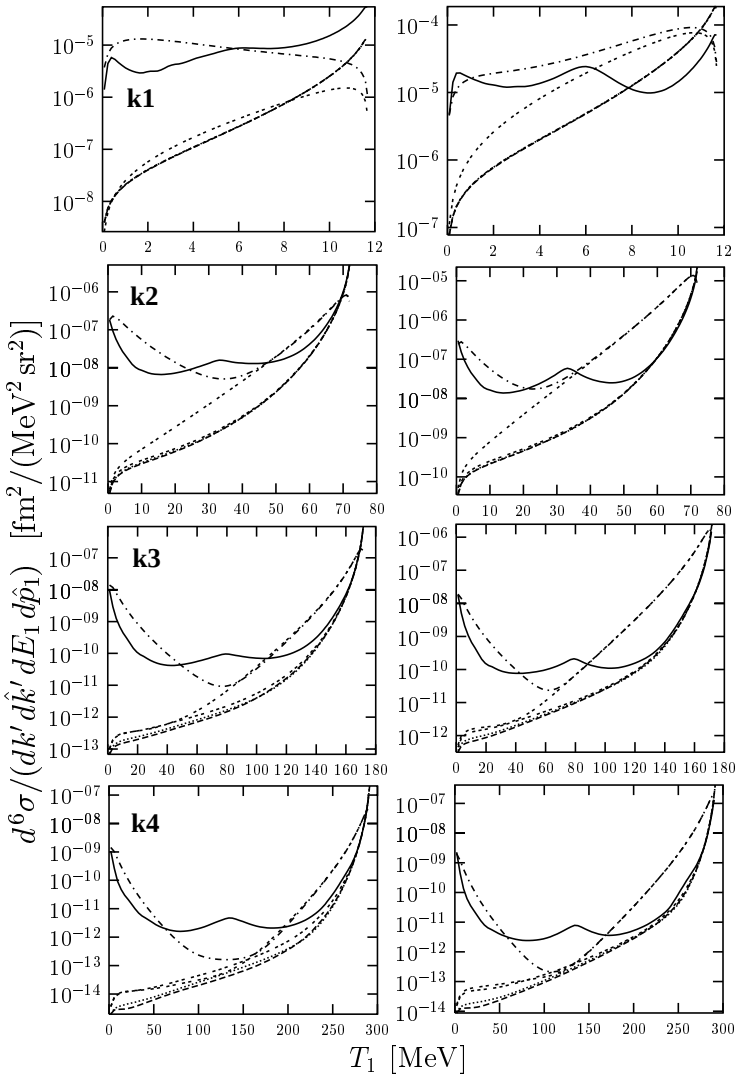

Fig. 8. The same as in Fig. 4 for the sixfold differential cross section.

Finally, in Figs. 8 and 9, we show the six fold differential cross sections for the neutron and proton knockout. Both, for the proton and neutron knockout, the cross sections vary by many orders of magnitude. There is always a very steep rise when the nucleon energy approaches its maximal value but the cross section for the proton case is always approximately factor 10 larger than the corresponding neutron observable. The PWIA and FSI23 predictions for small T_1 values are negligible and differ very much both from the PWIAS and results taking FSI fully into account. Except for the k1

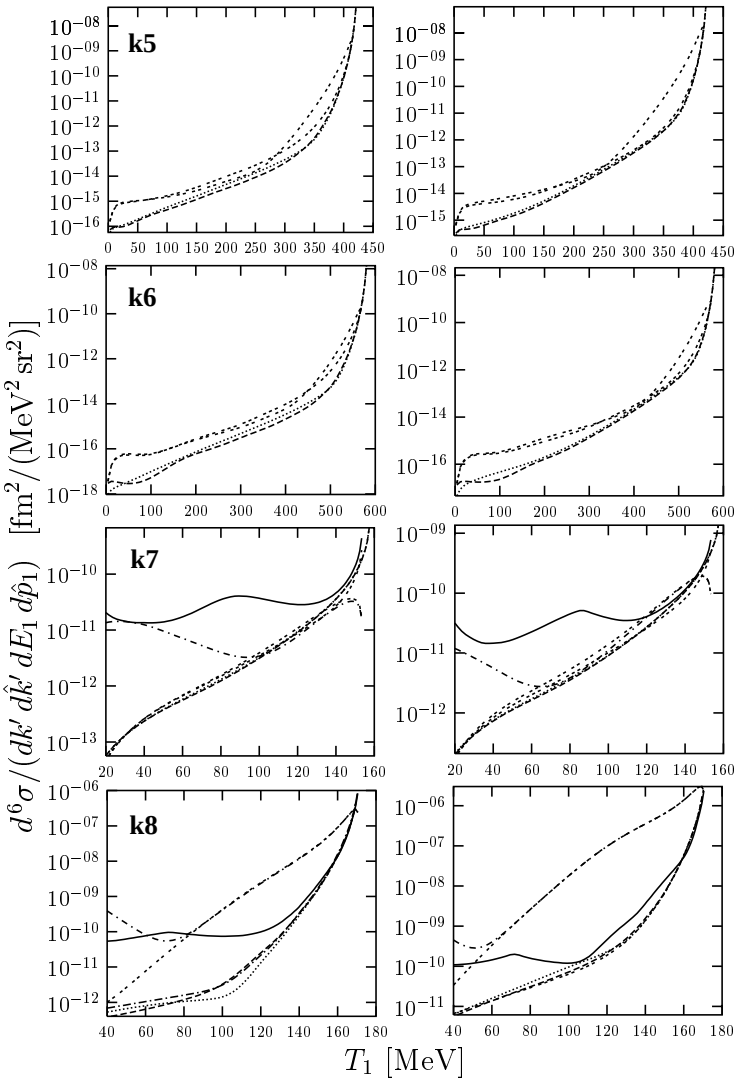

Fig. 9. The same as in Fig. 8 for the remaining four electron kinematics from Table I. The PWIAS prediction and the one with full FSI are missing for the k5 and k6 kinematics.

kinematics, we can always find an energy interval (at least on the logarithmic scale) where the group of the FSI23 lines is very close to the curve obtained with the full inclusion of FSI (when applicable). As expected, for the k5 and k6 kinematics the difference between the fully nonrelativistic and the other FSI23 results is best visible. The effects which we see for the k7 kinematics are magnified by the trivial differences in the allowed energy ranges.

4. Additional remarks on relativistic requirements

4.1. Requirements on the current

The components j^μ of the electromagnetic current operator have to obey the continuity equation, which can be translated into the well known form

$$[H, j^0(0)] = [\vec{P}, \vec{j}(0)]\,. \tag{59}$$

While this has been approximately fulfilled (using a single nucleon density in the lowest order of the p/m expansion) for instance in the form of the Riska prescription [32, 33] for a NN force like $AV18$ [34], a further requirement results from

$$e^{i\vec{\alpha}\cdot\vec{K}} j^\mu e^{-i\vec{\alpha}\cdot\vec{K}} = \Lambda^\mu_\nu j^\nu\,, \tag{60}$$

where $\vec{K}$ is the boost generator, which includes an interaction in the instant form of relativistic quantum mechanics. The vector $\vec{\alpha}$ is related to the relative velocity between inertial frames. This leads in infinitesimal form to the covariance conditions

$$[K^l, j^0(0)] = i\, j^l(0)\,, \tag{61}$$

$$[K^l, j^m(0)] = i\, \delta_{lm} j^0(0)\,. \tag{62}$$

Since K^l contains interactions j^l must contain on top of the single-body term at least two-body terms and in addition has to be consistent with the requirement from (59). Consequently (62) tells us that this must be true for j^0 as well. Thus if one enters into a kinematical regime where relativity plays a role the often used low energy assumption of a single-body density can no longer be valid. Apparently it is a difficult task phenomenologically to find currents which fulfill (59), (61) and (62).

For a single nucleon K^l and j^μ are known, of course, and fulfill the covariance equations. But even there it is a pretty complex interplay of kinematical variables to verify the conditions (61) and (62) as is obvious from the explicit expressions for the single nucleon matrix elements:

$$\begin{aligned}\langle \vec{p}s|K^l|\vec{p}'s'\rangle \;=\; & -\frac{i}{2}\left(\frac{p^{\,l}}{E_p} + 2E_p\nabla^l_p\right)\delta(\vec{p}-\vec{p}')\delta_{ss'} \\ & -\frac{1}{2}\frac{(\vec{p}\times\vec{\sigma})^l_{ss'}}{E-p+m}\delta(\vec{p}-\vec{p}')\,,\end{aligned} \tag{63}$$

$$\langle \vec{p}s|j^0|\vec{p}'s'\rangle = \frac{1}{2}\frac{1}{(2\pi)^3}\sqrt{\frac{E_p+m}{E_p}} \times \sqrt{\frac{E'_p+m}{E'_p}}\left(1+\frac{\vec{p}\cdot\vec{p}'+i\vec{\sigma}\cdot(\vec{p}\times\vec{p}')}{(E_p+m)(E'_p+m)}\right)_{ss'}, \tag{64}$$

$$\langle \vec{p}s|j^l|\vec{p}'s'\rangle = \frac{1}{2}\frac{1}{(2\pi)^3}\frac{1}{E_pE'_p} \times\left[\sqrt{\frac{E_p+m}{E'_p+m}}(p'^l+i(\vec{p}'\times\vec{\sigma})^l)+\sqrt{\frac{E'_p+m}{E_p+m}}(p^l-i(\vec{p}\times\vec{\sigma})^l)\right]_{ss'}. \tag{65}$$

The matrix elements (64) and (65) are consistent with (52) where we dropped for the sake of a simpler notation the nucleonic electromagnetic form factors. A very much more simple algebra is needed to verify (59) with $\langle \vec{p}s|H|\vec{p}'s'\rangle = E_p\delta(\vec{p}-\vec{p}')\delta_{ss'}$ and $\langle \vec{p}s|\vec{P}|\vec{p}'s'\rangle = \vec{p}\delta(\vec{p}-\vec{p}')\delta_{ss'}$.

The difficulty in fulfilling (59), (61) and (62) at the same time is illustrated in the Appendix. There we naively regard the standard two-body exchange current resulting from the one-pion exchange, the continuity equation and the assumption of a single nucleon density in lowest order of the p/m expansion. Now we use the lowest order form for the interaction in $\vec{K}$

$$\vec{K}_v = -iv\vec{\nabla}_{\vec{P}}\,, \tag{66}$$

where v is the two-body force in its center of mass frame and $\vec{P}$ the operator of total two-body momentum. This follows from the Poincaré algebra in the Bakamjian Thomas scheme. Then applying that vector interaction and using the same simple nucleon density the resulting right hand side of (61) does not coincide with the standard form of the exchange current as resulting from (59). Only for momentum transfer $\vec{Q} \equiv \vec{P}\,' - \vec{P}$ going to zero they agree. This indicates that a systematic p/m expansion is needed. But more importantly one needs a dynamical input for the charge density as well in order to fulfill the equations.

In a low momentum region where chiral perturbation theory can be used, the electromagnetic nucleonic current operator including two-body parts and more can be derived in the framework of effective field theory. Including relativistic corrections systematically should lead to currents and boost generators which fulfill the covariance equations as well as the continuity equation to a given order in the p/m expansion. Work in that direction is under way [35]. For a recent review on such an approach, however focusing on nuclear forces, see [36].

4.2. A low order 3N Hamiltonian in a moving frame

The approximation (21) for the boosted two-nucleon potential in Eq. (10) can be repeated with the $3N$ Hamiltonian in a moving frame (total $3N$ momentum $\vec{P}$ different from zero). It is given as

$$H = \sqrt{M^2 + P^2}\,, \tag{67}$$

where

$$M = M_0 + \sum_{i<j} V_{ij} + V_4\,, \tag{68}$$

is the $3N$ mass operator. Note V_{ij} is the boosted two-nucleon potential and V_4 is a $3N$ force. In this case the expansion in powers of $\vec{P}$ is even more justified than for the internal momentum $\vec{q}$ for the boosted two-body force, since $\vec{P}$ is controlled from outside. For example in the case of electron scattering on ^{3}He at rest it would be the momentum $\vec{Q}$ transferred from the electron. Let us assume that $\vec{P}$ is small enough that the expansion of H is justified. Then

$$H = M + \frac{P^2}{2M} + \dots\,, \tag{69}$$

$$\frac{1}{M} = \frac{1}{M_0} - \frac{1}{M_0}\left(\sum_{i<j} V_{ij} + V_4\right)\frac{1}{M_0}\,, \tag{70}$$

leading to

$$H = M_0 + \frac{P^2}{2M_0} + \sum_{i<j} V_{ij} + V_4 - \frac{P^2}{2}\frac{1}{M_0}\left(\sum_{i<j} V_{ij} + V_4\right)\frac{1}{M_0} + \dots\,. \tag{71}$$

Technically this is easy to handle since the corrections of $O(P^2)$ to the potentials are just multiplicative kinematical factors in momentum space.

5. Summary

Many important observables in electron induced breakup of ^{3}He are measured in kinematical regions, where a nonrelativistic approach is not applicable. Thus an approximation is needed with some relativistic features included, which can serve as a practical tool to analyze results of such experiments. One possibility is to extend the so-called FSI23 approximation (see Sec. 3) which has been used since many years to include some relativistic ingredients.

In this study we added to this approach a consistent relativistic treatment of the initial $3N$ bound state, the relativistic single nucleon current operator, the relativistic boosted NN scattering operator and relativistic kinematics. We studied a number of electron kinematics, mostly on a quasi-elastic scattering line, in order to estimate the effects of these new relativistic ingredients. We found out that the bulk of relativistic effects comes from the relativistic kinematics. Further (consistent with kinematics) relativistic features of the calculation are less important. For the kinematics within the shaded area of Fig. 3 (k1, k2, k3, k7, k8), even in the neighborhood of the highest energy of the ejected nucleon, the FSI23s and the full FSI are different. Therefore, the full FSI treatment is mandatory for a quantitative analysis. On top, especially for the k7 and k8 kinematics some relativistic effects are noticeable and should be included in the future analyzes of correspondingly precise data. For the kinematics k5 and k6 in the range of highest nucleon energies the relativistic effects are clearly visible, especially for neutron emission, and should be taken into account in the analysis of experimental data. Whether full FSI effects will be present there, too, cannot be answered by us right now. Nevertheless, as the first step the constructed approximate framework can be used to analyze experimental data taken at high energy and momentum transfers. In the future it should be replaced by fully relativistic calculations not available at the moment which include all FSI's along the lines of the approach applied in the $3N$ continuum in [21, 31]. In addition the current has to obey the continuum equation and the covariance equations consistently, which poses a nontrivial task.

This work was supported by the Polish State Committee for Scientific Research (KBN) under grant no. 2P03B00825. One of us (W.G.) would like to thank the Foundation for Polish Science for the financial support during his stay in Kraków. The numerical calculations have been performed on the IBM Regatta p690+ of the NIC in Jülich, Germany.

Appendix

Two-body terms

The two-body exchange current $\vec{j}_v$ related to the one-pion exchange

$$v = \frac{\vec{\sigma}_1 \cdot \vec{k}\, \vec{\sigma}_2 \cdot \vec{k}}{(\vec{k})^2 + (m_\pi)^2} \vec{\tau}_1 \cdot \vec{\tau}_2 \,, \tag{A.1}$$

has the well known form:

$$\langle \vec{p}\vec{P}|\vec{j}_v|\vec{p}'\vec{P}'\rangle = i(G_p - G_n)(\vec{\tau}_1 \times \vec{\tau}_2)_z \vec{\sigma}_1 \cdot \left(\vec{k} - \frac{\vec{Q}}{2}\right) \vec{\sigma}_2 \cdot \left(\vec{k} + \frac{\vec{Q}}{2}\right)$$
$$\times \left(\frac{1}{(\vec{k} - \frac{\vec{Q}}{2})^2 + (m_\pi)^2} - \frac{1}{(\vec{k} + \frac{\vec{Q}}{2})^2 + (m_\pi)^2}\right) \frac{\vec{k} + \frac{\vec{Q}}{2} - (\frac{\vec{Q}}{2} - \vec{q})}{(\vec{k} + \frac{\vec{Q}}{2})^2 - (\vec{k} - \frac{\vec{Q}}{2})^2}$$
$$- \left(\frac{\vec{\sigma}_2 \vec{\sigma}_1 \cdot (\vec{k} - \frac{\vec{Q}}{2})}{(\vec{k} - \frac{\vec{Q}}{2})^2 + (m_\pi)^2} + \frac{\vec{\sigma}_1 \vec{\sigma}_2 \cdot (\vec{k} + \frac{\vec{Q}}{2})}{(\vec{k} + \frac{\vec{Q}}{2})^2 + (m_\pi)^2}\right). \tag{A.2}$$

Here $G_{p(n)}$ are the proton (neutron) electric form factors, $\vec{Q} = \vec{P}' - \vec{P}$ and $\vec{k} = \vec{p} - \vec{p}'$. This result can be extracted from Eq. (59) in the form

$$\langle \vec{p}\vec{P}|[v, j^0]|\vec{p}'\vec{P}'\rangle =$$
$$\left[\frac{\vec{\sigma}_1 \cdot (\vec{k} - \frac{\vec{Q}}{2})\vec{\sigma}_2 \cdot (\vec{k} - \frac{\vec{Q}}{2})}{(\vec{k} - \frac{\vec{Q}}{2})^2 + (m_\pi)^2}) - \frac{\vec{\sigma}_1 \cdot (\vec{k} + \frac{\vec{Q}}{2})\vec{\sigma}_2 \cdot (\vec{k} + \frac{\vec{Q}}{2})}{(\vec{k} + \frac{\vec{Q}}{2})^2 + (m_\pi)^2})\right]$$
$$\times i(G_p - G_n)(\vec{\tau}_1 \times \vec{\tau}_2)_z \tag{A.3}$$
$$\equiv \vec{Q} \cdot \langle\, \vec{p}\vec{P}|\vec{j}_v|\vec{p}'\vec{P}'\rangle\,, \tag{A.4}$$

where the single nucleon density for proton (Π_p) and neutron (Π_n)

$$j^0 = j_1^0\Big(G_p\Pi_p(1) + G_n\Pi_n(1)\Big) + j_2^0\Big(G_p\Pi_p(2) + G_n\Pi_n(2)\Big) \tag{A.5}$$

has been used. In lowest order $\langle \vec{p}_1\vec{p}_2|j_1^0|\vec{p}_1'\vec{p}_2'\rangle = \delta(\vec{p}_2 - \vec{p}_2')$ and correspondingly for j_2^0. Now performing the same straightforward algebra using $\vec{K}_v$ from Eq. (66) leads to

$$\langle \vec{p}\vec{P}|[\vec{K}_v, j^0]|\vec{p}'\vec{P}'\rangle = i(G_p - G_n)(\vec{\tau}_1 \times \vec{\tau}_2)_z$$
$$\times i\vec{\nabla}_{\vec{Q}}\left(\frac{\vec{\sigma}_1 \cdot (\vec{k} + \frac{\vec{Q}}{2})\vec{\sigma}_2 \cdot (\vec{k} + \frac{\vec{Q}}{2})}{(\vec{k} + \frac{\vec{Q}}{2})^2 + (m_\pi)^2} - \frac{\vec{\sigma}_1 \cdot (\vec{k} - \frac{\vec{Q}}{2})\vec{\sigma}_2 \cdot (\vec{k} - \frac{\vec{Q}}{2})}{(\vec{k} - \frac{\vec{Q}}{2})^2 + (m_\pi)^2}\right). \tag{A.6}$$

Apparently $\langle \vec{p}'\vec{P}'|\vec{j}_v'|\vec{p}'\vec{P}'\rangle$ defined via

$$\langle \vec{p}\vec{P}|[\vec{K}_v, j^0]|\vec{p}'\vec{P}'\rangle \equiv i\langle \vec{p}'\vec{P}'|\vec{j}_v'|\vec{p}'\vec{P}'\rangle \tag{A.7}$$

is not the same as $\langle \vec{p}'\vec{P}'|\vec{j}_v|\vec{p}'\vec{P}'\rangle$ defined in Eq. (A.4) and given in Eq. (A3). They agree however for $\vec{Q} = 0$ as is easily seen.

REFERENCES

[1] A. Nogga, A. Kievsky, H. Kamada, W. Glöckle, L.E. Marcucci, S. Rosati, M. Viviani, *Phys. Rev.* **C67**, 034004 (2003) and references therein.

[2] W. Glöckle, H. Witała, D. Hüber, H. Kamada, J. Golak, *Phys. Rep.* **274**, 107 (1996).

[3] H. Witała *et al., Phys. Rev.* **C63**, 024007 (2001); J. Kuroś-Żołnierczuk *et al., Phys. Rev.* **C66**, 024003 (2002).

[4] J. Golak, R. Skibiński, H. Witała, W. Glöckle, A. Nogga, H. Kamada, *Phys. Rep.* **415**, 89 (2005).

[5] A. Deltuva, L.P. Yuan, J. Adam Jr., P.U. Sauer, *Phys. Rev.* **C70**, 034004 (2004).

[6] W. Xu *et al., Phys. Rev. Lett.* **85**, 2900 (2000).

[7] J. Golak, G. Ziemer, H. Kamada, H. Witała, W. Glöckle, *Phys. Rev.* **C63**, 034006 (2001); J. Golak, W. Glöckle, H. Kamada, H. Witała, R. Skibiński, A. Nogga, *Phys. Rev.* **C66**, 024008 (2002).

[8] J. Golak, W. Glöckle, H. Kamada, H. Witała, R. Skibiński, A. Nogga, *Phys. Rev.* **C65**, 044002 (2002).

[9] W. Xu *et al., Phys. Rev.* **C67**, 012201 (2003).

[10] W. Glöckle, H. Kamada, J. Golak, A. Nogga, H. Witała, R. Skibiński, J. Kuroś-Żołnierczuk, *Acta Phys. Pol. B* **32**, 3053 (2001).

[11] J. Golak, W. Glöckle, H. Kamada, H. Witała, R. Skibiński, A. Nogga, *Phys. Rev.* **C65**, 064004 (2002).

[12] J. Golak, R. Skibiński, H. Witała, W. Glöckle, A. Nogga, H. Kamada, *Phys. Rev.* **C72**, 054005 (2005).

[13] C. Carasco *et al., Phys. Lett.* **B559**, 41 (2003).

[14] H. Kamada, W. Glöckle, J. Golak, Ch. Elster, *Phys. Rev.* **C66**, 044010 (2002).

[15] F. Coester, *Helv. Phys. Acta* **38**, 7 (1965).

[16] W. Glöckle, T.-S. H. Lee, F. Coester, *Phys. Rev.* **C33**, 709 (1986).

[17] L. Müller, *Nucl. Phys.* **A360**, 331 (1981); W. Glöckle, L. Müller, *Phys. Rev.* C**23**, 1183 (1981).

[18] J. Carlson, V. R. Pandharipande, R. Schiavilla, *Phys. Rev.* **C47**, 484 (1993); J.L. Forest, V.R. Pandharipande, J.L. Friar, *Phys. Rev.* **C52**, 568 (1995); J.L. Forest, V.R. Pandharipande, J. Carlson, R. Schiavilla, *Phys. Rev.* **C52**, 576 (1995).

[19] H. Kamada, W. Glöckle, *Phys. Rev. Lett.* **80**, 2547 (1998).

[20] T.W. Allen, G.L. Payne, W.N. Polyzou, *Phys. Rev.* **C62**, 054002 (2000).

[21] H. Witała, J. Golak, W. Glöckle, H. Kamada, *Phys. Rev.* **C71**, 054001 (2005); H. Witała, J. Golak, R. Skibiński, *Phys. Lett.* **B634**, 374 (2006).

[22] S.J. Wallace, *Phys. Rev. Lett.* **87**, 180401 (2001).

[23] B.D. Keister, W.N. Polyzou, *Phys. Rev.* **C73**, 014005 (2006).

[24] W. Glöckle, *The Quantum Mechanical Few-Body Problem*, Springer-Verlag, Berlin 1983.

[25] D. Hüber, H. Kamada, H. Witała, W. Glöckle, *Few-Body Systems* **16**, 127 (1994).

[26] R. Machleidt, F. Sammarruca, Y. Song, *Phys. Rev.* **C53**, R1483 (1996).

[27] J. Golak, W. Glöckle, H. Kamada, H. Witała, R. Skibiński, A. Nogga, *Phys. Rev.* **C66**, 024008 (2002).

[28] G. Höhler, E. Pietarinen, I. Sabba-Stefanescu, F. Borkowski, G.G. Simon, V.H. Walther, R.D. Wendling, *Nucl. Phys.* **B114**, 505 (1976).

[29] T.W. Donnelly, A.S. Raskin, *Ann. Phys. (N.Y.)* **169**, 247 (1986).

[30] J. Golak, H. Witała, R. Skibiński, W. Glöckle, A. Nogga, H. Kamada, *Phys. Rev.* **C70**, 034005 (2004).

[31] R. Skibiński, H. Witała, J. Golak, `nucl-th/0604033`.

[32] D.O. Riska, *Phys. Scr.* **31**, 107 (1985).

[33] D.O. Riska, *Phys. Scr.* **31**, 471 (1985).

[34] R.B. Wiringa, V.G.J. Stoks, R. Schiavilla, *Phys. Rev.* **C51**, 38 (1995).

[35] E. Epelbaum, private communication.

[36] E. Epelbaum, *Prog. Part. Nucl. Phys.* **57**, 654 (2006).